THE JOURNAL OF BIOLOGICAL CHEMISTRY VOL. 290, NO. 3, pp. 1885–1897, January 16, 2015

Parkinsonism-associated Protein DJ-1/Park7 Is a Major Protein Deglycase That Repairs Methylglyoxal- and Glyoxal-glycated Cysteine, Arginine, and Lysine Residues

Received for publication, July 17, 2014, and in revised form, November 20, 2014 Published, JBC Papers in Press, November 21, 2014, DOI 10.1074/jbc.M114.597815

Gilbert Richarme[‡1], **Mouadh Mihoub**[‡], **Julien Dairou**[§], **Linh Chi Bui**[§], **Thibaut Leger**[¶], **and Aazdine Lamouri**[‖]

From the [‡]*Stress Molecules, Institut Jacques Monod, Université Paris 7, CNRS UMR 7592, 75013 Paris, France, the* [§]*Université Paris Diderot, Sorbonne Paris Cité, Unité de Biologie Fonctionnelle et Adaptative UMR 8251 CNRS, Bioprofiler Facility, F-75205, Paris, France, the* [¶]*Proteomics Facility, Institut Jacques Monod, Université Paris 7, CNRS, UMR 7592, 75013 Paris, France, and the* [‖]*Université Paris Diderot, Sorbonne Paris Cite, ITODYS, UMR 7086 CNRS, 75013 Paris, France*

Background: Protein glycation is a nonenzymatic covalent reaction between proteins and carbonyl groups resulting in protein denaturation.
Results: DJ-1 is the first protein deglycase that repairs proteins from glycation by glyoxals, which constitutes most glycation damage.
Conclusion: DJ-1 is a novel protein repair enzyme that protects proteins against glycation.
Significance: DJ-1 deglycase activity changes our view on glycation/deglycation and DJ-1-associated Parkinsonism.

Glycation is an inevitable nonenzymatic covalent reaction between proteins and endogenous reducing sugars or dicarbonyls (methylglyoxal, glyoxal) that results in protein inactivation. DJ-1 was reported to be a multifunctional oxidative stress response protein with poorly defined function. Here, we show that human DJ-1 is a protein deglycase that repairs methylglyoxal- and glyoxal-glycated amino acids and proteins by acting on early glycation intermediates and releases repaired proteins and lactate or glycolate, respectively. DJ-1 deglycates cysteines, arginines, and lysines (the three major glycated amino acids) of serum albumin, glyceraldehyde-3-phosphate dehydrogenase, aldolase, and aspartate aminotransferase and thus reactivates these proteins. DJ-1 prevented protein glycation in an *Escherichia coli* mutant deficient in the DJ-1 homolog YajL and restored cell viability in glucose-containing media. These results suggest that DJ-1-associated Parkinsonism results from excessive protein glycation and establishes DJ-1 as a major anti-glycation and anti-aging protein.

The Parkinsonism-associated protein DJ-1/Park7 is described as a multifunctional oxidative stress response protein that belongs to the PfpI/Hsp31/DJ-1 superfamily, whose members possess a conserved exposed cysteine involved in environmental stress resistance (1–3). DJ-1 has been reported to function as a chaperone for synuclein (4, 5), a covalent chaperone for the thiol proteome (6, 7), a peroxidase (8), a protease (9), a glyoxalase (10), a stabilizer of Nrf2 (11), an apoptosis inhibitor via interaction with Daxx (12), and a translational regulator (13, 14).

We reported recently that DJ-1 formed mixed disulfides with sulfenylated proteins and released repaired proteins following the reduction of mixed disulfides by low molecular weight thiols (6, 7). The ability of DJ-1 to repair covalently modified proteins, the fact that its presumed chaperone, protease, and glyoxalase activities are weaker than those of major chaperones, proteases, and glyoxalases (3, 9, 10), the finding that enzymes involved in protein repair, such as thioredoxins and peptidyl prolyl isomerases, display chaperone properties (15–17), and the co-expression of the *Bacillus subtilis* DJ-1 homolog YraA with the aldoketoreductase AdhA, which is involved in carbonyl stress resistance (18), suggested to us that DJ-1 might be involved in glycated protein repair.

The nonenzymatic reaction between sugar carbonyl groups and amino acids was discovered by the French chemist Louis Camille Maillard in 1912 (19). This reaction also occurs *in vivo* (20) and involves the spontaneous reaction of endogenous and exogenous carbonyls with the thiol and amino groups of proteins, nucleic acids and amino lipids (21). The condensation reaction between carbonyls and amino acids begins with the rapid formation of a hemithioacetal with cysteines and formation of aminocarbinols with arginines and lysines (21, 22), after which a series of dehydrations, oxidations, and rearrangements leads to a myriad of products, including Schiff bases, Amadori products, advanced glycation end products (AGEs),[2] and protein cross-links (21). Mechanisms to protect the cells against carbonyl/electrophile stress involve aldoketoreductases, which reduce carbonyls into alcohols (23); glyoxalases, which degrade glyoxals into acid-alcohols (24, 25); detoxification systems that form and export electrophile-glutathione conjugates (26), and fructosamine-3-kinases (FN3Ks), which, by phosphorylating lysine-fructosamines formed after Amadori rearrangement of protein lysines glycated by glucose, increase their rate of deglycation by a factor of three and release repaired proteins and

[1] To whom correspondence should be addressed: Stress Molecules, Inst. Jacques Monod, Université Paris 7, CNRS UMR 7592, 15 Rue Hélène Brion, 75013 Paris, France. Tel.: 33-1-57-27-80-57; Fax: 33-1-57-27-81-01; E-mail: richarme@paris7.jussieu.fr.

[2] The abbreviations used are: AGE, advanced glycation end product; MGO, methylglyoxal; GO, glyoxal; CML, carboxymethyl lysine; G-H1, *N*-(5-hydro-4-imidazolon-2-yl)ornithine; MG-H1, *N*-(5-hydro-5-methyl-4-imidazolon-2-yl)ornithine; FN3K, fructosamine-3-kinase; FBP, fructose-1,6-biphosphate; RP, reverse phase; DTNB, 5,5′-dithiobis(nitrobenzoic acid).

3-deoxyglucosone (27). Moreover, FN3K-related enzymes deglycate lysines glycated by ribose-5-phosphate and erythrose-4-phosphate, and prokaryotic amadoriases and fructosamine-6-kinases deglycate free lysine-fructosamines for metabolic purposes (26). Here, we show that DJ-1 is a major protein deglycase that repairs methylglyoxal- and glyoxal-glycated amino acids and proteins and releases deglycated proteins and lactate or glycolate, respectively.

EXPERIMENTAL PROCEDURES

DJ-1 Expression and Purification—The DJ-1 gene was amplified by PCR from a human kidney cDNA library and inserted into the expression plasmid pET-21a, and this recombinant plasmid was introduced into *Escherichia coli* strain BL21 (DE3) (7, 9). DJ-1 was purified as described previously (28). The C106S, C53S, and C46S DJ-1 mutants were expressed using recombinant pET-21a plasmids (7, 9) and purified as described previously (28).

Deglycation of N-Acetylcysteine, N-Acetylarginine, and N-Acetyllysine—Experiments were performed at 22 °C in N_2-gassed 50 mM sodium phosphate buffer, pH 7.0. Glycation of NacCys by MGO and its deglycation by DJ-1 were monitored by hemithioacetal absorbance at 288 nm (29) and reverse phase (RP)-HPLC. Glycation/deglycation of NacArg and NacLys was followed by RP-HPLC: 80 mM NacArg was incubated at 22 °C in 150 μl of buffer with 80 mM MGO. After 40 min, the mixture was incubated with 4 μM DJ-1. Lactate was analyzed with D- and L-lactate dehydrogenases. For RP-HPLC, samples were injected into a Kromasil Eternity C18 column at 40 °C (for Cys and Lys) or a PrimeSep 200 column (for Arg). Mobile phase for isocratic elution (Cys and Lys) consisted of 25 mM monobasic sodium phosphate, 0.3 mM of the ion-pairing agent 1-octane sulfonic acid, and 4% (v/v) methanol at pH 2.7 adjusted with 85% phosphoric acid. For Arg experiments, the same mobile phase was used, and elution was achieved with a 4–10% methanol gradient. Column chromatography experiments were performed twice and produced similar results. For the measure of kinetic constants, glycated *N*-acetylcysteine, *N*-acetylarginine (from the 1.9-min peak in Fig. 1*H*), and N-acetyllysine were prepared by RP-HPLC and used immediately for K_m and k_{cat} determination. The results are the mean values of three experiments (S.E. was less than 15%).

Deglycation of BSA, GAPDH, Fructose 1,6-Biphosphate Aldolase, and Aspartate Aminotransferase—Experiments were performed in N_2-gassed 50 mM sodium phosphate buffer (pH 7.0). Glycation/deglycation of BSA cysteine was followed by DTNB titration (30). BSA (700 μM) was incubated with 100 mM MGO for 110 min at 37 °C, separated by gel filtration on a Bio-Gel P2, and incubated at 22 °C in the absence or presence of DJ-1. Glycation/deglycation of GAPDH was followed by measurement of GAPDH activity (30) and titration of thiol groups. GAPDH from rabbit muscle (300 μM monomers) was incubated with 5 mM MGO at 22 °C for 40 min, separated from MGO by gel filtration, and incubated in the absence or presence of DJ-1. In experiments where DJ-1 was added to the initial glycation mixtures, GAPDH activity was measured by adding 5 μl of a 100-fold diluted glycation mixture to a cuvette containing 150 μl of substrates. Glycation/deglycation of BSA lysines was followed by measuring the absorbance at 333 nm (31). BSA was incubated in buffer at 22 °C in the absence or presence of 6 mM MGO and DJ-1, as indicated. MGO concentrations were measured with 2,4-dinitrophenylhydrazine (10), and lactate concentrations were determined using L- or D-lactate dehydrogenase. BSA arginines were measured using phenanthrenequinone (32). Glycation/deglycation of fructose bisphosphate aldolase A (from rabbit muscle; EC 4.1.2.13; Sigma) and aspartate aminotransferase (from pig heart, cytoplasmic; EC 2.6.1.1; Sigma) were followed by measuring enzymatic activities (33, 34), by detecting the glycated forms with anti-AGE antibodies (Cell Biolabs Inc.), and by mass spectrometry. Deglycation experiments were performed at least three times, and representative results are shown.

Measurement of MGO or GO Levels and Lactate or Glycolate Formation—DJ-1, MGO, or GO was added to N_2-gassed 50 mM sodium phosphate buffer, pH 7.0, at 22 °C in a total volume of 70 μl. To measure the disappearance of MGO or GO, the reaction was stopped by the addition of 10 μl of reaction mixture to 120 μl of 0.1% 2,4-dinitrophenylhydrazine solution. The solution was incubated for 15 min at 22 °C, 160 μl of 10% NaOH was added, and absorbance was measured after 15 min at 540 nm for MGO and 570 nm for GO. The appearance of lactate was measured using L- or D-lactate dehydrogenase (35). Glycolate formation was measured by RP-HPLC (10). The results are the mean values of three experiments (S.E. was less than 15%).

Bacterial Strains, Bacterial Extracts, and Immunoblotting—The wild-type *E. coli* strain BL21 (DE3), the *yajL* mutant, and these two strains supplemented with the plasmids pCA24N-*yajL* and pET21a-*DJ-1* (7) were grown overnight in Luria broth supplemented with 0.6% glucose. YajL and DJ-1 were induced with 1 mM isopropyl β-D-thiogalactopyranoside. Bacterial lysates were prepared by ultrasonic disruption of bacteria resuspended at $A_{600} = 100$ in 50 mM sodium phosphate, pH 7.0, and 50 mM NaCl. For immunoblotting with anti-AGE antibodies, 3,000 g of supernatants of bacterial lysates (10 μg) or purified proteins (0.2 μg, unless otherwise indicated) were separated by SDS-PAGE. Proteins were transferred to a nitrocellulose membrane and probed with anti-AGE antibodies, following the manufacturer's protocol (Cell Biolabs Inc.). Rabbit anti-YajL antibodies were prepared by Eurogentec, using purified YajL from our laboratory, and rabbit anti-DJ-1 antibodies were obtained from Abcam. For measuring cell viability, cultures were serially diluted from 10^2 to 10^6 and spotted (4 μl) onto LB plates, and growth was observed after 20 h of incubation at 30 °C. For the fluorescent analysis of total *E. coli* protein, the *yajL* mutant and the *yajL* mutant transformed with pET21a-*DJ-1* (induced with isopropyl β-D-thiogalactopyranoside at $A_{600} = 0.8$) were grown at 37 °C in LB medium. At $A_{600} = 1.2$ (late exponential phase), MGO was added to half of the samples, and bacterial lysates were prepared at the indicated times after treatment. Lysates were dialyzed for 3 h against 50 mM sodium phosphate buffer, pH 7.0, and incubated for 48 h at 22 °C, and fluorescence (excitation at 350 nm, emission at 440 nm) was measured at a protein concentration of 0.5 mg/ml using an F-2000 Hitachi fluorometer. Bovine serum albumin at 0.5 mg/ml was used as a standard. Viability experiments, AGE

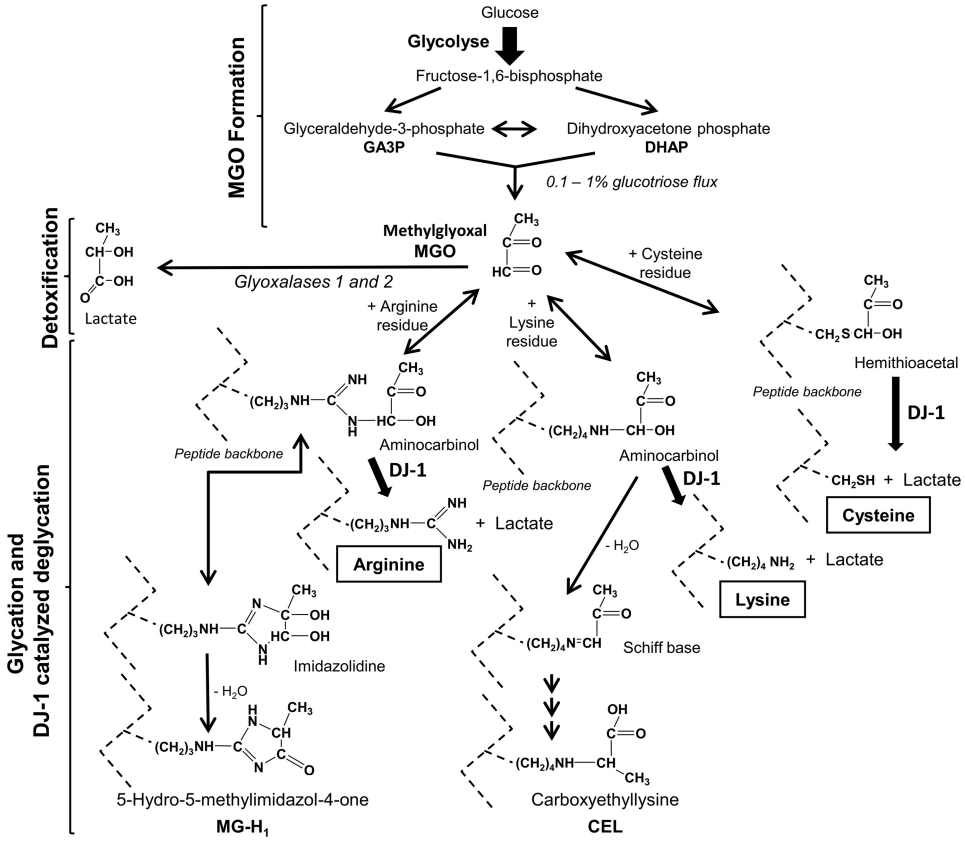

SCHEME 1. **Methylglyoxal metabolism, protein glycation by methylglyoxal, and deglycation by DJ-1/Park7.** MGO forms spontaneously as a glycolytic by-product and is detoxified by the sequential action of glyoxalases 1 and 2. It forms covalent adducts with cysteines, arginines, and lysines (hemithioacetals with cysteines and aminocarbinols with arginines and lysines) and also forms imidazolidines with the arginine guanidino group. Hemithioacetals, aminocarbinols, and imidazolidines are transformed into intermediate glycation products (such as Schiff bases) and AGEs, including MG-H1 and carboxyethyllysine (*CEL*), and are also transformed into cross-link products such as methylglyoxal-lysine dimers (MOLD; not shown). DJ-1, as described in this paper, transforms hemithioacetal (via a thioester) into cysteine and lactate, and aminocarbinols (via an amide) into arginine/lysine and lactate, and in this way prevents the formation of Schiff bases and AGEs. Glyoxal (CHO-CHO) is formed by lipid peroxidation and the degradation of saccharides and glycated proteins and is detoxified by glyoxalases (not shown). Glyoxal and methylglyoxal form similar glycation adducts, and the main glyoxal-derived AGEs are G-H1, carboxymethyllysine and glyoxal-lysine dimers (GOLD) (not shown). DJ-1 also repairs glyoxal-glycated proteins and produces glycolate (CH_2OH-COOH) instead of lactate.

detection experiments, and protein fluorescence analysis were performed three times; representative results are shown.

Mass Spectrometry—Aliquots (2 μg) of samples (FBP aldolase and glyoxal, FBP aldolase, glyoxal, and DJ-1) were digested overnight in solution at 37 °C with GluC protease (12.5 μg/ml; Sigma) in 20 mM sodium phosphate buffer, pH 7.8, containing 10% acetonitrile. Digests were analyzed in triplicate by an LTQ Velos Orbitrap mass spectrometer equipped with an EASY-Spray nanoelectrospray ion source and coupled to an EASY-nLC Proxeon 1000 chromatographic system (Thermo Fisher Scientific). Parameters used for peptides separation and mass spectrometry were as described previously (36). Label-free quantification was performed on raw data with Progenesis-LC software 4.1 (Nonlinear Dynamics). Peptide identification was performed with an in-house Mascot search server (Matrix Science, Boston, MA). The following modifications were used in dynamic modifications: oxidation (M), glyoxal (CKR), dehydrated-glyoxal (CKR), and deamidation (N, Q). The maximum number of missed cleavages by GluC was limited to two. Mass tolerance was set to 7 ppm for precursor ions and 0.5 Dalton for fragments. MS/MS data were searched against an *Oryctolagus cuniculus* database extracted from the NCBInr database. After the results were imported into Progenesis-LC software, and normalization of peptide abundances based on FBP peptides only was applied. Peptides with ion scores of less than 20 were rejected. Peptides with glyoxal or derived modifications and an analysis of variance score of less than 0.05 were considered.

RESULTS

Methylglyoxal and Glyoxal Metabolism

In addition to being an environmental toxin, methylglyoxal forms spontaneously from triosephosphates in all organisms (Scheme 1) and in minor amounts from threonine and acetone. Glyoxal is formed by lipid peroxidation and the degradation of saccharides and glycated proteins (21). The cellular concentrations of methylglyoxal and glyoxal are in the ranges 1–5 and 0.1–1 μM, respectively (21). Methylglyoxal and glyoxal are detoxified into lactate and glycolate, respectively, by the sequential action of glyoxalases 1 and 2 (24, 25) (Scheme 1), as well as by aldoketoreductases and efflux pumps (23, 26).

Methylglyoxal and glyoxal are potent glycating agents that form covalent adducts with cysteines, arginines, and lysines. With regard to the activity of methylglyoxal, reaction with a cysteine residue results in the rapid formation of a hemithioacetal, reaction with a lysine residue produces the aminocarbinol

lysinemethylglyoxal glycosylamine, and reaction with an arginine residue forms the aminocarbinol arginine methylglyoxal glycosylamine and a 4,5-dihydroxy-5-methylimidazolidine derivative (Scheme 1). The lysine and arginine derivatives undergo dehydratation and/or rearrangement, which slowly lead to the formation of intermediate and AGEs, including Schiff bases, MG-H1 (derived from arginine), and carboxyethyllysine (Scheme 1). Protein glycation by glyoxal proceeds via similar reactions, producing the AGEs G-H1 (derived from arginine) and carboxymethyllysine (Lys-NH-CH_2-COOH; not shown). The bifunctional carbonyls of methylglyoxal and glyoxal form cross-linked products, such as MOLD (methylglyoxal-lysine dimer) and GOLD (glyoxal-lysine dimer). Degradation of hemithioacetals and aminocarbinols by DJ-1 (Scheme 1), as described in the present work, prevents the formation of these AGEs.

DJ-1 Deglycates Cysteine, Arginine, and Lysine

N-Acetylcysteine Deglycation—We incubated equimolar concentrations of methylglyoxal and *N*-acetylcysteine for 2 min to form the hemithioacetal adduct (the product of the first reaction described below), which is detectable by its absorbance at 288 nm (29). We investigated hemithioacetal degradation in the presence of DJ-1 by measuring the decrease in absorbance at 288 nm and analyzing the reactants on a C18 RP-HPLC column (Fig. 1, *A–C*). The hemithioacetal was stable but exhibited a half-time of 30 min in the presence of 4 μM DJ-1 (Fig. 1, *A* and *B*). The K_m and k_{cat} of cysteine deglycation at 22 °C were 0.3 mM and 0.4 s^{-1} respectively (Table 1). Hemithioacetal degradation resulted in the quantitative formation of *N*-acetylcysteine and lactate (Fig. 1, *B–D*). Lactate analysis with L- and D-lactate dehydrogenases showed that NacCys deglycation produced 67% L-lactate and 33% D-lactate (Fig. 1*D*). The following reactions are likely to have occurred.

$$\text{NacCys-SH} + \text{CHO-CO-CH}_3 \rightarrow \text{NacCys-S-CHOH-CO-CH}_3$$

(Spontaneous hemithioacetal formation)

$$\text{NacCys-S-CHOH-CO-CH}_3 \rightarrow \text{NacCys-S-CO-CHOH-CH}_3$$

(H migration is catalyzed by DJ-1, reminiscent of glyoxalase 1)

$$\text{NacCys-S-CO-CHOH-CH}_3 \rightarrow \text{NacCys-SH} + \text{COOH-CHOH-CH}_3$$

(Thioester hydrolysis is catalyzed by DJ-1, reminiscent of glyoxalase 2.)

REACTIONS 1–3

Thus, DJ-1 degrades the hemithioacetal formed between *N*-acetylcysteine and methylgloxal into *N*-acetylcysteine and a 67/33 mixture of L- and D-lactate.

N-Acetyllysine Deglycation—We next incubated equimolar concentrations of NacLys and methylglyoxal for 40 min to form glycated NacLys, which is composed primarily of the aminocarbinol NacLys methylglyoxal glycosylamine, the product of the first reaction written below (29). RP-HPLC analysis of the glycation mixture after incubation shows the NacLys peak and the glycated NacLys peak. When the glycation mixture was incubated with 4 μM DJ-1, the glycated NacLys peak decreased, whereas the NacLys peak increased (Fig. 1, *E* and *F*), and quantitative formation of L-lactate occurred (Fig. 1, *D* and *F*). Thus, DJ-1 deglycates glycated *N*-acetyllysine into *N*-acetyllysine and lactate. The reactions likely to have occurred are described below in the paragraph dealing with NacArg.

N-Acetylarginine Deglycation—To form glycated NacArg, we incubated equimolar concentrations of NacArg and methylglyoxal for 40 min. Under similar conditions, Lo *et al.* (29) reported formation of the aminocarbinol NacArg-methylglyoxal glycosylamine (the product of the first reaction written below) and the imidazolidine formed by reaction of the ketone group of the aminocarbinol with the arginine imino group (Scheme 1). RP-HPLC analysis (PrimeSep200) of the glycation mixture (Fig. 1*H*) revealed a NacArg peak, a major NacArgglc peak (at 3.0 min) that likely contains the aminocarbinol formed with the arginine NH_2, plus the corresponding imidazolidine, and a minor NacArgglc peak (at 1.9 min) that possibly contains the aminocarbinol formed with the arginine δ-NH group (see below). When the glycation mixture was incubated with 4 μM DJ-1, the two glycated NacArg peaks decreased, whereas the NacArg peak increased (Fig. 1, *H* and *I*), and quantitative formation of L-lactate occurred (Fig. 1, *D* and *I*). However, whereas degradation of the NacArgglc (aminocarbinol 2) eluting at 1.9 min was rapid (~1 h, as with the degradation of NacCysglc and NacLysglc; Fig. 1*G*), degradation of NacArgglc eluting at 3.0 min displayed biphasic kinetics, with a rapid initial phase (which likely corresponds to degradation of aminocarbinol 1), and a slow exponential phase lasting several hours ($\tau_{1/2} = 2.8$ h, corresponding to a catalytic constant of $0.7 \times 10^{-4}\ s^{-1}$ at pH 7.0, 22 °C). The slow phase fits with degradation of the aminocarbinol formed upon displacement of the imidazolidine-aminocarbinol equilibrium, whose catalytic constant was reported to be $1.9 \times 10^{-4}\ s^{-1}$ at pH 7.4 and 37 °C (29). For the degradation of aminocarbinols, the following reactions are likely to have occurred.

For NacArg, an aminocarbinol can also form with the arginine δ-NH group and imidazolidines by further reaction of aminocarbinols with the arginine imino group (Scheme 1).

$$\text{NacArg/Lys-NH}_2 + \text{CHO-CO-CH}_3 \rightarrow \text{NacArg/Lys-NH-CHOH-CO-CH}_3$$

(Spontaneous aminocarbinol formation occurs on the NH_2 group)

$$\text{NacArg/Lys-NH-CHOH-CO-CH}_3 \rightarrow \text{NacArg/Lys-NH-CO-CHOH-CH}_3$$

(H migration is catalyzed by DJ-1, reminiscent of glyoxalase 1)

$$\text{NacArg/Lys-NH-CO-CHOH-CH}_3 \rightarrow \text{NacArg/Lys-NH}_2 + \text{COOH-CHOH-CH}_3$$

(Amidolysis is catalyzed by DJ-1, reminiscent of peptidase activity.)

REACTIONS 4–6

These results suggest that DJ-1 degrades aminocarbinol intermediates formed upon arginine (or lysine) glycation by methylglyoxal, with the quantitative release of arginine (or lysine)

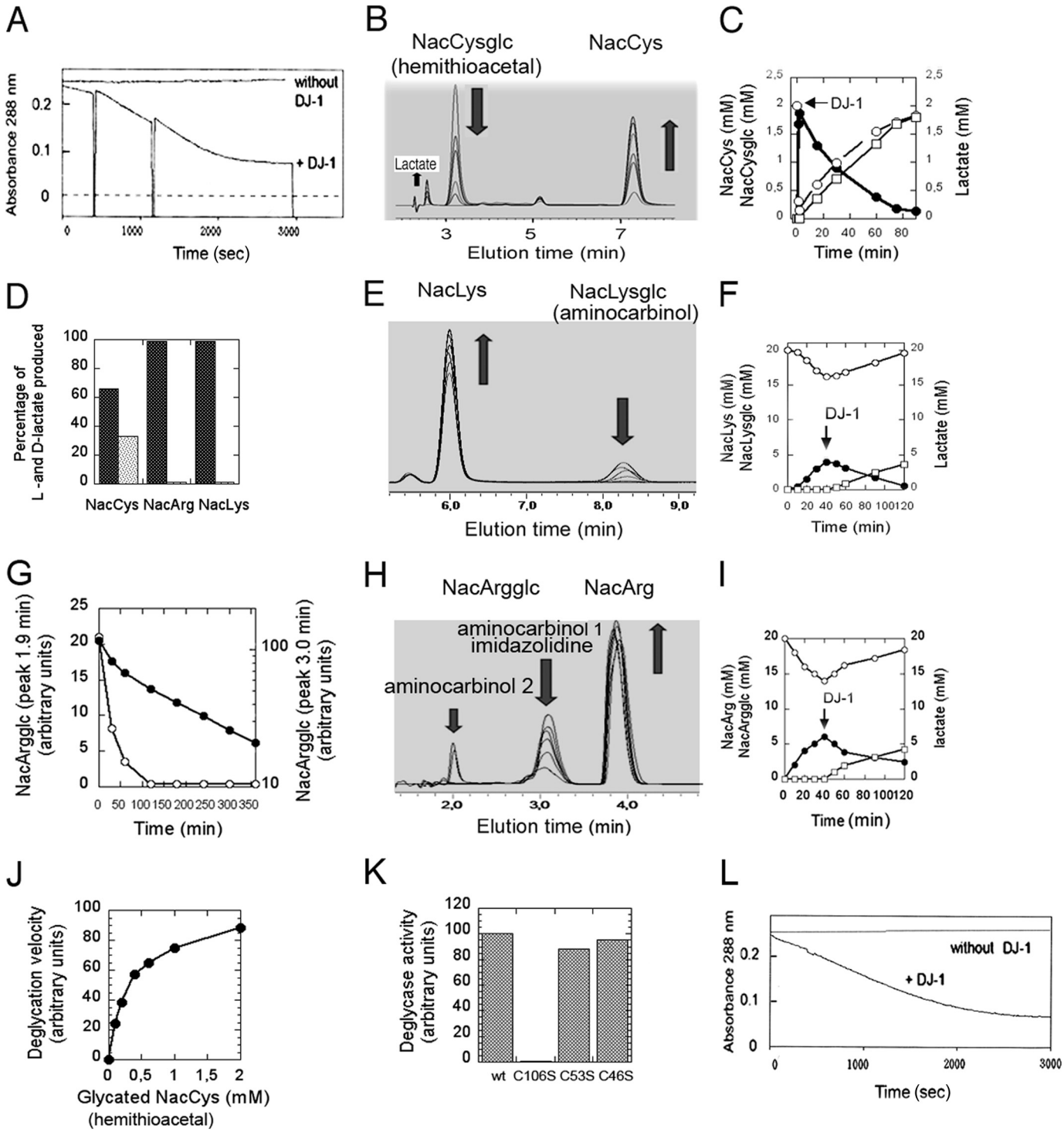

FIGURE 1. **Deglycation of *N*-acetylcysteine, *N*-acetylarginine, and *N*-acetyllysine.** *A*, NacCys and MGO (2 mM each) were incubated for 2 min, resulting in formation of the hemithioacetal, which absorbs light a 288 nm. DJ-1 (2 μM) was added to one sample at 0, 300, and 1100 s. *B*, *E*, and *H*, NacCys and MGO (2 mM each; *B*), NacArg and MGO (80 mM each; *E*), or NacLys and MGO (80 mM each; H) were incubated for 2 min (*B*) and 40 min (*E* and *H*), respectively, after which 4 μM DJ-1 was added to the glycation mixture (*B*) or to the 4-fold diluted glycation mixture (*E* and *H*). The amounts of Nac amino acids and glycated Nac amino acids were analyzed by RP-HPLC at various time points after DJ-1 addition. *C*, *F*, and *I*, the amounts of Nac amino acids, glycated Nac amino acids, and lactate were determined during glycation/deglycation experiments. MGO was added to Nac amino acids at time 0, allowing glycation to occur, and 4 μM DJ-1 was added as indicated to initiate deglycation. Nac amino acids (*open circles*) and glycated Nac amino acids (*filled circles*) were determined by RP-HPLC (as described for *B*, *E*, and *H*), and lactate was assessed using lactate dehydrogenases. *D*, the relative amounts of L-lactate (*black columns*) and D-lactate (*gray columns*) produced during deglycation of NacCys, NacArg, and NacLys by DJ-1 were analyzed using L- and D-lactate dehydrogenases. *G*, degradation kinetics of NacArgglc (peak eluting at 1.9 min (*open symbols*) and peak eluting at 3.0 min (*closed symbols*)). *J*, dependence of the rate of deglycation of the hemithioacetal formed between *N*-acetylcysteine and MGO on its concentration. A value of 100 represents a rate of 1.26 μmol/min/mg of DJ-1. *K*, deglycase activity of DJ-1 and the C106S, C53S, and C46S mutants were assayed for deglycation of the hemithioacetal formed between *N*-acetylcysteine and MGO. *L*, glutathione and MGO (2 mM each) were incubated for 15 min, resulting in formation of a thiohemiacetal that absorbs light at 288 nm, after which 4 μM DJ-1 was added to one sample at time 0.

TABLE 1
Catalytic constants of the deglycation by DJ-1 of glycated *N*-acetylcysteine, *N*-acetylarginine, and *N*-acetyllysine at 22 °C in 50 mM sodium phosphate buffer, pH 7.0

Catalytic constant	*N*-Acetylcysteine	*N*-Acetylarginine	*N*-Acetyllysine
K_m (mM)	0.32	0.44	0.35
k_{cat} (s^{-1})	0.42	0.27	0.28

and L-lactate. They also suggest that DJ-1, by displacing the imidazolidine-aminocarbinol equilibrium, allows indirect degradation of imidazolidine intermediates before they convert into irreversible AGEs, such as MG-H1, MG-H2, and MG-H3. Thus, in contrast with known deglycases, which only deglycate lysines (27), DJ-1 deglycates cysteines, arginines, and lysines, the three major glycated amino acids.

Catalytic Constants of DJ-1 and Importance of Cys^{106}

We measured the catalytic constants of the deglycation of glycated *N*-acetylcysteine, *N*-acetylarginine, and *N*-acetyllysine by DJ-1 (Fig. 1*J* and Table 1). The K_m and k_{cat} of the three reactions were similar (~0.4 mM for the K_m and 0.3 s^{-1} for the k_{cat} at 22 °C), suggesting that DJ-1 principally recognizes the glycated portion of these molecules. Moreover, these k_{cat} values were in the same range as those of other enzymes involved in protein folding or repair, such as GroEL and thioredoxins (16, 17).

The crystal structure of DJ-1 combined with phylogenetic analysis and physiological studies underscored the importance of cysteine 106 in its function (1–3, 5), whereas Cys^{53} and Cys^{46} appear to play secondary roles. We investigated *N*-acetylcysteine deglycation by C106S, C53S, and C46S DJ-1 mutants and found that the C106S mutant was inactive, whereas the two other mutants displayed activities similar to those of wild-type DJ-1 (Fig. 1*K*). Thus, Cys^{106} is the nucleophile crucial for the deglycase activity of DJ-1.

DJ-1 Deglycates Glutathione and Protein Cysteines

We incubated equimolar concentrations of methylglyoxal and glutathione for 15 min to form the hemithioacetal adduct, which was detectable by its absorbance at 288 nm. The hemithioacetal was stable in the absence of DJ-1 but disappeared with a half-time of 30 min in the presence of 4 μM DJ-1 (Fig. 1*L*). Thus, although glutathione is not required as a co-factor for DJ-1, glycated glutathione, like glycated cysteine, constitutes a DJ-1 substrate.

BSA contains a single exposed cysteine (Cys^{34}, titratable by DTNB) involved in oxidative stress protection. DJ-1 can repair this cysteine from sulfenylation (6). After BSA treatment with methylglyoxal for 110 min at 37 °C, the number of BSA-titrated cysteines decreased from 0.62 to 0.28 (Fig. 2*A*). We separated BSA from MGO by gel permeation chromatography and incubated 300 μM BSA at 22 °C, either alone or in the presence of 3 μM DJ-1. After addition of DJ-1, the titratable cysteines of BSA increased from 0.28 to 0.52 with a half-time of 2 min; in contrast, they remained constant in the absence of DJ-1 or in the presence of 5 mM glutathione (Fig. 2*A*). Thus, DJ-1 deglycates the exposed cysteine of BSA with a k_{obs} of 0.3 s^{-1}.

GAPDH performs covalent catalysis with its active site cysteine 150 (30). GAPDH activity decreased by 80% in the presence of 5 mM MGO, whereas DTNB-titrated cysteines decreased from 1.9 to 1.1, reflecting the covalent reaction of the active site cysteine with MGO (30) (Fig. 2*B*). We then separated GAPDH from MGO by gel permeation chromatography and incubated 60 μM GAPDH, either alone or in the presence of 2 μM DJ-1. In the absence of DJ-1, GAPDH activity decreased further, to 10% of its initial activity, whereas in its presence, it increased to 50% of its initial activity, with a half-time of 2 min. DTNB-titrated cysteines increased from 1.1 to 1.6 with similar kinetics. Thus, DJ-1 reactivates GAPDH by deglycating its active site cysteine. When 2 μM DJ-1 was added to the initial glycation mixture, GAPDH activity did not decrease, suggesting that DJ-1 deglycates GAPDH as glycation occurs, thereby preventing formation of deglycation-resistant intermediates. Moreover, when added to the initial glycation mixture, 2 μM DJ-1 fully protected 300 μM GAPDH against glycation by 5 mM glyoxal (Fig. 2*C*).

Remarkably, compared with *in vivo* concentrations, the concentrations of MGO and GO are >1000-fold higher (5 mM *versus* 1–5 μM for MGO and 0.1–1 μM for GO (25)), substrate protein concentrations are 9-fold lower (11 mg/ml GAPDH *versus* 100 mg/ml total cytoplasmic protein (25)), and DJ-1 concentrations are similar (2 μM in our experiment *versus* ~1 μM in skin, 10 μM in brain, and 40 μM in liver). Thus, DJ-1 efficiently deglycates proteins *in vitro*, even though the workload is markedly heavier than *in vivo*.

DJ-1 Prevents Schiff Base Formation between Serum Albumin Lysines and MGO, but Does Not Degrade Schiff Bases

When proteins react with methylglyoxal, they exhibit an increase in light absorption between 300 and 400 nm, which can be attributed to the formation of Schiff base linkages between lysine side chains and MGO. (The initially formed aminocarbinol Lys-NH-CHOH-CO-CH_3 dehydrates in minutes to hours to form the Schiff base Lys-N=CH-CO-CH_3 (31) (Scheme 1)). When 70 μM BSA was incubated with 6 mM MGO for 3 h, its absorption spectrum displayed a shoulder between 300 and 370 nm. Remarkably, the shoulder was considerably lower when 3 μM DJ-1 was present in the BSA/MGO mixture (Fig. 2*D*). In samples containing 70 μM BSA, 6 mM MGO, and 1.5 or 3 μM DJ-1, the rate of Schiff base formation was reduced by several-fold compared with samples without DJ-1 (Fig. 2*E*), whereas the concentration of MGO decreased by less than 12% in 60 min. This result suggests that the anti-glycation effect of DJ-1 does not result from MGO depletion but instead from its deglycase activity; moreover, in samples containing MGO and DJ-1 (or MGO and BSA), the MGO concentration did not decrease significantly, suggesting that MGO depletion correlates with BSA deglycation (see below).

In contrast with its ability to prevent Schiff base formation, DJ-1 did not degrade Schiff bases. We glycated 70 μM BSA by treatment with 6 mM MGO for 2 h and then incubated glycated BSA (separated from MGO by gel permeation chromatography) with 4 μM DJ-1. We observed no decrease in BSA absorbance at 333 nm over 90 min, suggesting that DJ-1 was unable to deglycate Schiff bases (not shown). The ability of DJ-1 to

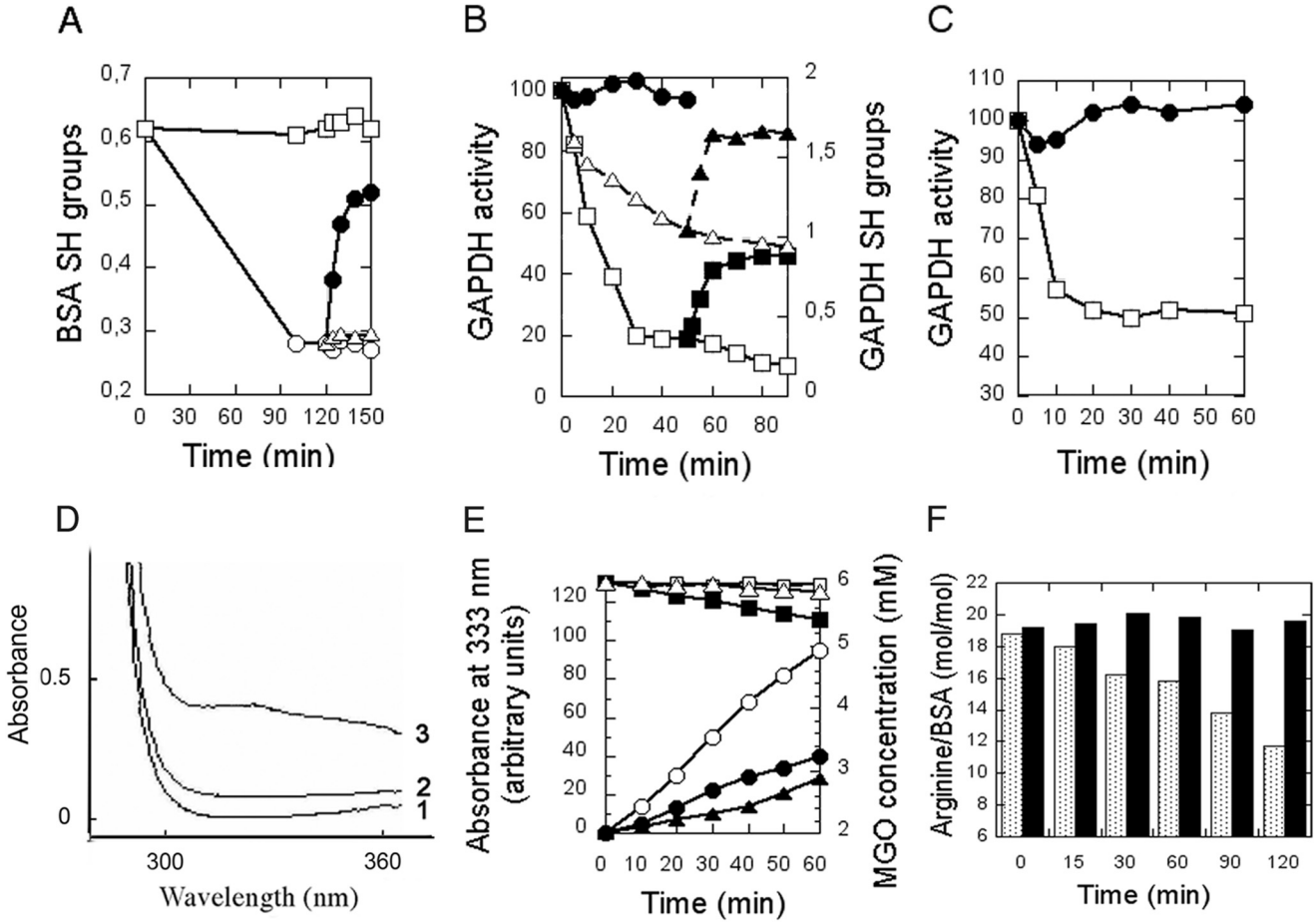

FIGURE 2. **Deglycation and reactivation of serum albumin and glyceraldehyde-3-phosphate dehydrogenase.** *A*, BSA was incubated with MGO over a period of 120 min, separated from MGO by gel permeation chromatography, and incubated in the absence (*open circles*) or presence (*filled circles*) of 3 μM DJ-1 or in the presence of 5 mM glutathione (*open triangles*). *Squares* represent BSA SH groups without MGO treatment. *B*, GAPDH was incubated with MGO, and GAPDH activity (*open squares*) and SH groups (*open triangles*) were assayed at different times. At 40 min, GAPDH was separated from MGO by gel permeation chromatography, incubated in the absence (*open symbols*) or presence (*filled symbols*) of DJ-1, and GAPDH activity (*squares*) and SH groups (*triangles*) were assayed. In a separate experiment, DJ-1 was added to the initial glycation mixture, and GAPDH activity was assayed (*filled circles*). *C*, GAPDH was incubated with GO in the absence (*open squares*) or presence (*filled circles*) of DJ-1, and GAPDH activity was assayed at different times. *D* and *E*, prevention of Schiff base formation between BSA lysines and MGO. *D*, BSA was incubated with MGO in the absence (*curve 3*) or presence of DJ-1 (*curve 2*), and the absorption spectra were recorded; The spectrum of BSA without MGO treatment is displayed in *curve 1*. *E*, BSA was incubated with MGO in the absence of DJ-1 (*open circles*) or presence of 1.5 μM (*filled circles*) or 3 μM (*filled triangles*) DJ-1. A value of 100 represents an $A = 0.1$. MGO consumption by BSA, MGO, and 1.5 μM DJ-1 (*filled squares*); BSA and MGO (*open squares*); and MGO and 1.5 μM DJ-1 (*open triangles*) was measured. *F*, deglycation of BSA arginines; BSA was incubated with MGO in the absence (*gray columns*) or presence of DJ-1 (*black columns*), and free arginines were titrated at various times.

prevent Schiff base formation, but not to degrade them, is consistent with its ability to degrade the aminocarbinol (Schiff base precursor). Consequently, the designation of Schiff bases (which form in hours) and Amadori products (which form in days) as early glycation intermediates should be revisited, because for DJ-1 these compounds represent late intermediates, whereas hemithioacetals and aminocarbinols, which form in seconds to minutes, represent early intermediates.

DJ-1 Deglycates Serum Albumin Arginines

Arginine is a major target of glycation by dicarbonyl compounds including methylglyoxal, with the initial formation of arginine-methylglyoxal glycosylamine, followed by dihydroxyimidazolidine, which is slowly dehydrated to produce arginine-derived hydroimidazolone MG-H1 (Scheme 1), the major methylglyoxal-derived AGE (25, 29). When 500 μM BSA was incubated at 37 °C with 20 mM MGO for 2 h, its titratable arginines decreased from 18.8 to 13.2 per BSA molecule as a consequence of arginine glycation, whereas they remained constant when 5 μM DJ-1 was added to the glycation mixture (Fig. 2*F*). Thus, DJ-1 efficiently deglycates BSA cysteines, lysines, and arginines.

DJ-1 Deglycates FBP Aldolase and Aspartate Transaminase

The active site of rabbit muscle FBP contains three lysines (Lys^{42}, Lys^{108}, and Lys^{230}) and three arginines (Arg^{43}, Arg^{149}, and Arg^{303}). As previously reported (33), 15 μM FBP was rapidly inactivated by 10 mM MGO (Fig. 3*A*). DJ-1 (4 μM) prevented (when added to the initial glycation mixture), stopped (when added after 10 min), or partially reversed (when added after 20 min) this inactivation (Fig. 3*A*). FBP was also inactivated by 5 mM GO, and 4 μM DJ-1 completely prevented this inactivation (Fig. 3*B*). As shown in Fig. 3*C*, in which aldolase was revealed with anti-AGE antibodies, DJ-1 afforded full protection against glycation of aldolase by glyoxal.

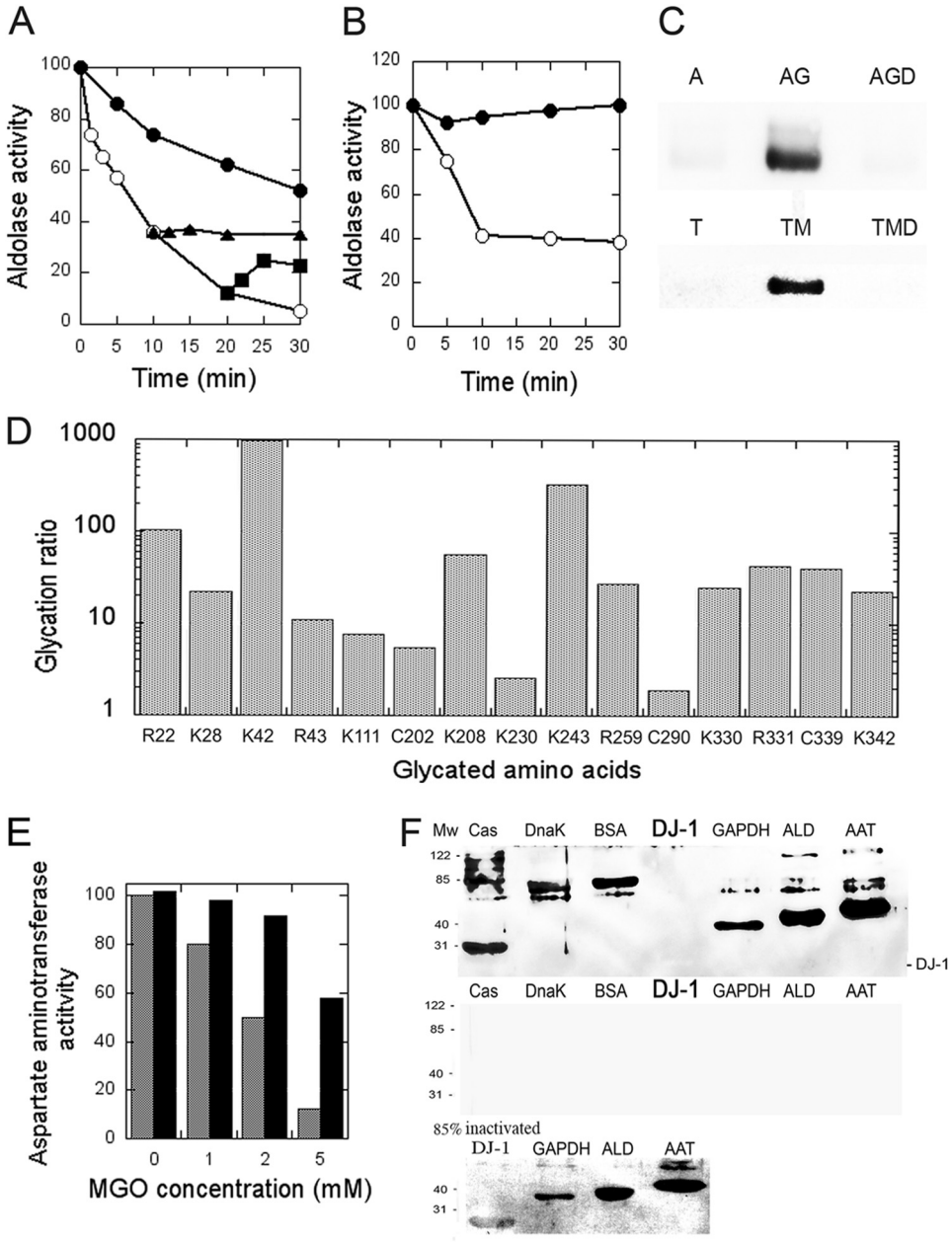

FIGURE 3. **Deglycation of aldolase and aspartate aminotransferase.** *A* and *B*, aldolase activity was measured after incubation with MGO (*A*) or GO (*B*), in the absence (*open circles*) or presence of DJ-1 added to the initial glycation mixture (*filled circles*) or after 10 min (*filled triangles*) or 20 min (*filled squares*). *C*, glycation of aldolase and aspartate aminotransferase was assayed by immunoblotting with anti-AGE antibodies: commercial enzymes (*A* and *T*), aldolase glycated by GO for 30 min in the absence (*AG*) or presence (*AGD*) of DJ-1 (in conditions described in *B*), and aspartate aminotransferase glycated for 30 min by 2 mM MGO in the absence (*TM*) or presence (*TMD*) of DJ-1. *D*, mass spectrometry analysis of aldolase deglycation by DJ-1. Fructose bisphosphate aldolase (20 μM) was glycated for 1 h by 5 mM glyoxal in the absence or presence of 5 μM DJ-1, separated from glyoxal by gel permeation chromatography, and analyzed by mass spectrometry. The glycation ratio is the ratio between glycation levels in the absence or presence of DJ-1. *E*, aspartate aminotransferase activity was measured after incubation for 30 min with MGO, before (*gray columns*) and again after an additional 2 min reactivation by DJ-1 (*black columns*). *F*, DJ-1 deglycation. Seven proteins were incubated with MGO and probed with anti-AGE antibodies (*top panel*). The same proteins were incubated without MGO and probed with anti-AGE antibodies (*middle panel*). A DJ-1 preparation that had lost 85% of its deglycase activity (as judged by its ability to deglycate *N*-acetylcysteine hemithioacetal) and three other proteins were incubated with MGO in the same conditions as above and probed with anti-AGE antibodies (*bottom panel*).

Aldolase glycation was also analyzed by mass spectrometry. DJ-1 prevented glycation of Arg^{22}, Lys^{28}, Lys^{42}, Arg^{43}, Lys^{111}, Cys^{202}, Lys^{208}, Lys^{230}, Lys^{243}, Arg^{259}, Cys^{290}, Lys^{318}, Lys^{330}, Arg^{331}, Cys^{339}, and Lys^{342} (Fig. 3*D* and Table 2); glycation ratios in the absence or presence of DJ-1 ranged from 1.9 for Cys^{290} and 2.6 for Lys^{230} (two buried residues) to 330 for Lys^{243} and 980 for Lys^{42}. The median glycation ratio was 25, reflecting the efficiency of DJ-1 in the presence of high glyoxal concentrations. Lys^{42}, Arg^{43}, and Lys^{230} are located in the active site, with Lys^{42} and Arg^{43} being involved in substrate binding (mutation of Arg^{43} results in 14-fold decrease in activity) and Lys^{230} forming a Schiff base with the substrate (mutation of Lys^{230} results in complete loss of activity). These results confirm that DJ-1 prevents glycation of cysteines, arginines, and lysines.

The active site of cytoplasmic aspartate aminotransferase contains two arginines involved in aspartate binding and a

TABLE 2

Mass spectrometry analysis of fructose bisphosphate aldolase deglycation by DJ-1

20 μM aldolase was glycated for 1 h by 5 mM glyoxal in the absence of presence of 5 μM DJ-1, separated from glyoxal by gel permeation and analyzed by mass spectrometry. Glycation ratio is the ratio between glycation levels in the absence or presence of DJ-1.

Sequence of glycated peptide	Modification and position in peptide	Amino acid	Glycation ratio	Analysis of variance	Mascot score
IAHRIVAPGKGILAADE	Glyoxal (Arg^4)	Arg^{22}	102	3.70E-05	23.93
LSDIAHRIVAPGKGILAADE	Glyoxal (Lys^{13})	Lys^{28}	22	1.71E-06	40.01
STGSIAKRLQSIGTENTEE	Glyoxal (Lys^7)	Lys^{42}	980	1.12E-05	43.52
STGSIAKRLQSIGTENTEE	Glyoxal (Arg^8)	Arg^{43}	11	2.73E-03	38.45
KGVVPLAGTNGE	Glyoxal (Lys^1)	Lys^{111}	7.7	0.000105	75.07
LKRCQYVTE	Glyoxal (Cys^4)	Cys^{202}	5.4	3.14E-05	22.75
KVLAAVYKALSD	Glyoxal (Lys^1)	Lys^{208}	56	0.00995	47.56
GTLLKPNMVTPGHACTQKYSHEE	Glyoxal (Lys^5)	Lys^{230}	2.6	7.51E-05	22.41
	Glyoxal (Lys^{18})	Lys^{243}	330	1.02E-02	27.07
IAMATVTALRRTVPPAVTGVTFLSGGQSEEE	Glyoxal (Arg^{11})	Arg^{259}	27	0.000572	27.79
ASINLNAINKCPLLKPWALTFSYGRAL	Glyoxal (Cys^{11})	Cys^{290}	1.9	0.0286	21.28
YVKRALANSLACQGKYTPSGQAGAAASE	Glyoxal (Lys^3)	Lys^{330}	25	0.0016	45.9
	Glyoxal (Arg^4)	Arg^{331}	43	5.41E-05	22.83
	Glyoxal (Cys^{12})	Cys^{339}	40	0.00195	38.72
	Glyoxal (Lys^{15})	Lys^{342}	23	2.43E-06	62.1

lysine that forms a transient covalent bond with pyridoxal phosphate. As reported previously (34), aspartate aminotransferase (10 μM) activity was decreased by 20–90% by 1–5 mM methylglyoxal at 37 °C (Fig. 3*E*). The addition of 2 μM DJ-1, 30 min after the addition of MGO, rapidly restored (in 2 min) up to 90–100% of aspartate aminotransferase activity following 1–2 mM methylglyoxal stress and up to 60% after 5 mM methylglyoxal stress (Fig. 3*E*). As shown in Fig. 3*C*, DJ-1 afforded full protection against glycation by 2 mM methylglyoxal.

DJ-1 Deglycation

We incubated seven proteins (β-casein, DnaK, BSA, DJ-1, GAPDH, fructose biphosphate aldolase, and aspartate aminotransferase; 0.8 μg each) separately with 5 mM MGO for 4 h at 37 °C and assessed their glycation status using anti-AGE antibodies. All proteins, except DJ-1, reacted with anti-AGE antibodies (Fig. 3*F*, *top panel*), suggesting that they were glycated, especially because they did not react with anti-AGE antibodies in the absence of MGO treatment (Fig. 3*F*, *middle panel*). The lack of reaction between DJ-1 and anti-AGE antibodies is likely a result of DJ-1 deglycase activity, especially because a DJ-1 preparation that had lost 85% of its deglycase activity reacted with anti-AGE antibodies (Fig. 3*F*, *bottom panel*).

The Previously Reported Glyoxalase Activity of DJ-1 Reflects Its Deglycase Activity

DJ-1 has been reported to function as a glutathione-independent glyoxalase, displaying a 1,000-fold lower activity than the glutathione-dependent glyoxalases Glo1 and Glo2 (10). We demonstrate below that the apparent glyoxalase activity of DJ-1 reflects its deglycase activity. First, the kinetics of MGO degradation (at micromolar DJ-1 concentrations) displayed a lag, which was likely required for spontaneous formation of the substrate, glycated DJ-1 or glycated BSA. Duration of the lag ranged from 40 min at 1 μM DJ-1 to 5 min at 8 μM DJ-1 and 1 min in the presence of 15 μM BSA (Fig. 4*A*). Second, the apparent glyoxalase activity of DJ-1 increased in a linear fashion with the square of DJ-1 concentration, in accordance with DJ-1 being both an enzyme (deglycase) and a substrate (glycated DJ-1) (Fig. 4*B*). DJ-1 was dimeric at all concentrations tested, suggesting that this did not result from a monomer-dimer equilibrium with an active dimer (not shown) (37). Third, the negligible levels of apparent glyoxalase activity of DJ-1 (1.5 μM) were strongly stimulated by BSA, with an apparent K_a of ~5 μM BSA (Fig. 4*C*). Stimulation by BSA was also observed when glyoxal was used as a glycating agent (Fig. 4*C*), and the amounts of glycolate produced were similar to those of GO consumed (not shown). These results are consistent with DJ-1 substrates being glycated proteins (DJ-1 or BSA in this section) instead of glyoxals, in accordance with the results presented above.

DJ-1 Protects Cells against Protein Glycation and Loss of Viability in Glucose-containing Media

E. coli contains three DJ-1 homologs, YajL, YhbO, and HchA, which are involved in resistance to environmental stresses (7, 28, 38–41) including carbonyl stress. YajL is the closest DJ-1 homolog, with YajL and DJ-1 displaying 40% sequence identity and a similar three-dimensional structure (42). In addition, the *yajL* mutant displayed the highest sensitivity to carbonyl stress.[3] Glycation affects bacteria under standard laboratory conditions, leading to a decline in viability during the stationary phase, and the addition of excess glucose or methylglyoxal results in increased loss of viability (43). The *yajL* mutant (but not the parental strain) suffered from a 100-fold decrease in viability after incubation for 48 h in LB medium containing 0.6% glucose, and the mutant was rescued by YajL- and DJ-1-overproducing plasmids (Fig. 4*D*).

We also investigated the glycation status of protein extracts by probing immunoblots with anti-AGE antibodies. The wild-type strain displayed a small quantity of glycated proteins after overnight culture in LB medium supplemented with 0.6% glucose, whereas the *yajL* mutant displayed much higher levels of glycated proteins (Fig. 4, *E* and *F*). Protein glycation in both the wild-type strain and the *yajL* mutant was reduced when DJ-1 was expressed in these strains (Fig. 4, *E* and *F*).

We investigated further the effect of DJ-1 expression on glycation of the *yajL* mutant under basal and methylglyoxal stress conditions by examining the fluorescent properties of total protein isolated from *E. coli* cells (glycated proteins display

[3] G. Richarme, M. Mihoub, and V. Gautier, unpublished results.

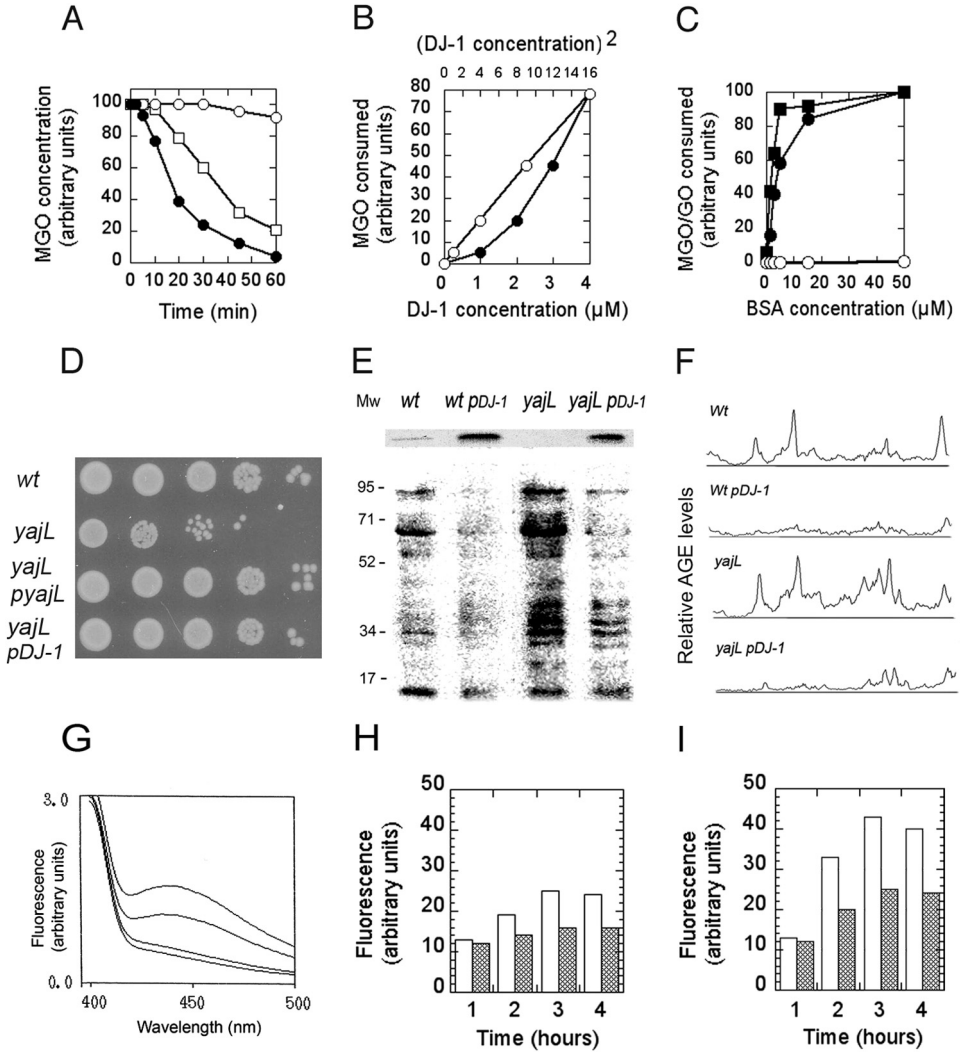

FIGURE 4. **DJ-1 kinetics and protection against viability loss and cellular glycation.** *A*, kinetics of decreasing MGO levels. MGO (2 mM) was incubated with 1 μM DJ-1 (*open circles*), 8 μM DJ-1 (*open squares*), or 8 μM DJ-1 and 15 μM BSA (*filled circles*). A value of 100 represents 2 mM MGO. *B*, the rate of decrease or MGO *versus* DJ-1 concentration. DJ-1 was incubated for 30 min in the presence of 1.5 mM MGO, and MGO levels were measured (a value of 80 represents 200 μM MGO). MGO levels are represented as a function of DJ-1 concentration (*filled circles*) or of the square of DJ-1 concentration (*open circles*). *C*, BSA stimulation. DJ-1 (1.5 μM) was incubated for 20 min with 1.5 mM MGO (*filled circles*) or GO (*filled squares*) in the presence of BSA at the indicated concentrations (*open circles* represent assays with BSA and MGO alone), and MGO or GO levels were measured (a value of 100 represents a rate of 200 μM of MGO or GO consumed in 20 min). *D*, bacteria were grown until the stationary phase in LB medium containing 0.6% glucose and left under agitation and aeration at 37 °C for 48 h in the same medium. A 4-μl aliquot of bacteria was serially diluted from 10^2 to 10^6 and spotted on LB plates for viability determination. *E*, bacterial lysates (10 μg) from the wild-type strain, the wild-type strain transformed with the DJ-1 expression plasmid, the *yajL* mutant, and the *yajL* mutant transformed with the DJ-1 expression plasmid were probed with anti-AGE antibodies. The expression of YajL and DJ-1 monitored by immunoblotting 10 μg of lysates from the *wt* strain and *yajL* mutant with anti-YajL antibodies and from the DJ-1 expressing strains with anti-DJ-1 antibodies is shown at the top of the figure. *F*, densitometric scans of glycated proteins distribution of extracts displayed in *E*. Quantification was performed with ImageJ software. *G*, fluorescence emission spectra (λ_{ex} = 350 nm) from *bottom* to *top* of buffer, native bovine serum albumin, and protein extracts from the *yajL* mutant expressing DJ-1 and the *yajL* mutant in samples obtained 3 h after treatment with 2 mM MGO. *H* and *I*, fluorescence of total *E. coli* protein extracted from the *yajL* strain (*white columns*) or the *yajL* strain expressing DJ-1 (*gray columns*) at different times after reaching a bacterial density of 1.2 at 600 nm (late exponential phase). MGO (2 mM) was added to bacteria at time 0 in experiment displayed in *I*.

increased fluorescence ($Ex_{350\ nm}$) in the 400–500-nm range (44). DJ-1 expression resulted in decreased protein glycation of the *yajL* mutant (Fig. 4*G*), both in the absence of exogenous carbonyl stress (DJ-1 alleviated the increase in protein glycation observed during the transition to the stationary phase of growth (44) (Fig. 4*H*)) and after the induction of stress with 2 mM methylglyoxal (Fig. 4*I*).

DISCUSSION

The literature on DJ-1 should be reconsidered in view of its deglycase activity.

DJ-1 Deglycase—To execute its deglycase activity, DJ-1 recruits its previously reported biochemical functions: (i) chaperone activity (4, 5, 28) to interact with non-native glycated proteins and gain access to partially buried glycated sites; (ii) glyoxalase 1 activity (10, 21) to interact with glycated substrates and convert hemithioacetals into thioesters, and aminocarbinols into amides; (iii) reactive cysteine 106 with a depressed pK_a of 5.4 (3, 7), to attack carbonyl groups of thioesters and amides; (iv) glyoxalase 2 activity (10, 21) to cut thioesters for cysteine deglycation; and (v) amidase/peptidase activity (9, 45) to cut amide bonds for lysine/arginine deglycation.

Glutathione and Electrophile Stress—Whereas glutathione performs multiple roles in electrophile stress resistance, acting as a co-enzyme of glyoxalases and glutathione-dependent aldehyde dehydrogenases, a covalent acceptor of carbonyl compounds, and a substrate of glutathione *S*-transferases and multidrug resistance transporters (as a glutathione-electrophile conjugate), it is surpassed by DJ-1 for protein deglycation: glutathione is rather inefficient at degrading glycosylamines (Schiff bases) by transglycating glucose to itself (47), and in our hands, it was unable to deglycate cysteine and BSA. DJ-1 does not require glutathione as a co-factor; however, glycated glutathione constitutes a DJ-1 substrate, suggesting that DJ-1 may be involved in sanitizing the glutathione pool.

Neurodegenerative Diseases—The deglycase activity of DJ-1 suggests that DJ-1-associated Parkinsonism results from excessive protein glycation, which affects dopaminergic transmission in the *substantia nigra*. It also strengthens the role of protein glycation in the etiology of neurodegenerative diseases (48). Protein glycation promotes the deposition of proteins, because of protein denaturation and formation of protease-resistant cross-links, and increases protein aggregation in Alzheimer, Parkinson, and Huntington diseases. The extent of Tau, β-amyloid, synuclein, and huntingtin glycation is correlated with the pathologies of the patients (48). Moreover, glycation is responsible, via the AGE receptor, for an increase in oxidative stress and inflammation through the formation of reactive oxygen species and activation of NF-κB (49). In Alzheimer disease, the AGE receptor also stimulates the transport of β-amyloid across the blood brain barrier into the brain (49).

Glycation/Deglycation—The discovery of the deglycase activity of DJ-1 is a major advance in glycation research. Whereas scavengers involved in degradation and export of electrophiles (aldoketoreductases, glyoxalases, glutathione/glutathione *S*-transferases/efflux pumps) are relatively efficient, FN3Ks display more moderate functions in electrophile stress resistance (21, 27). Compared with FN3Ks, DJ-1 appears to be an overachiever: (i) its specific activity is 20,000-fold higher (k_{obs} expressed in s^{-1} instead of d^{-1}); (ii) it deglycates cysteines, arginines, and lysines (instead of only lysines); (iii) it deglycates all proteins tested; (iv) it operates immediately after glycation onset (whereas FN3K acts after the Amadori rearrangement); (iv) it releases innocuous products (lactate and glycolate) instead of dicarbonyl 3-deoxyglucosone; (v) it does not require any co-factors (whereas FN3K requires ATP); and (vi) in accordance with its efficiency, DJ-$1^{-/-}$ mice display Parkinson disease-type abnormalities and metabolic defects (3), whereas Fn3k$^{-/-}$ mice are healthy (although they do display higher levels of free and protein-bound fructosamines (27). Nevertheless, fructosamine-3-kinases and related enzymes are involved in defense against glycation by glucose, ribose-5-phosphate and erythrose-4-phosphate, whereas DJ-1 reverses glycation by glyoxals, which suggests that these enzymes possess complementary functions in providing protection against carbonyl stress. However, because glyoxals are by-products of carbohydrate metabolism, DJ-1 is also involved in preventing sugar-dependent glycation. Both sugars and dicarbonyls cause important glycation damage, with sugars being more concentrated than dicarbonyls (millimolar range instead of micromolar range) but less active (methylglyoxal is 24,000-fold more potent as a glycating agent than glucose (21)). If we consider the clinical urinary excretion of glycation free adducts by type 1 diabetic subjects, fructoselysine represents 22 nmol/mg creatinine, whereas adducts mainly derived from glyoxals-dependent glycation (carboxymethyllysine, carboxyethyllysine, G-H1, and MG-H1) represent 42 nmol/mg creatinine (22).

Consideration of the characteristics of DJ-1 deglycase changes our views on glycation and deglycation. First, it shortens the time scale of deglycation. Because DJ-1 catches glycation in the act, it appears that everything is settled at the onset of glycation, when it is still time for DJ-1-catalyzed deglycation. Consequently, with respect to glycation by dicarbonyl compounds, "late" should describe minutes or hours after glycation onset (29, this work) rather than days, months, or years after, as is often assumed. Second, hemithioacetals and aminocarbinols (DJ-1 substrates) that form immediately upon glycation, which are tacitly evoked in many glycation reviews (however, see Ref. 29 for a description of their formation) could be upgraded from a merely implicit status to the rank of early glycation products. Schiff bases, which form in minutes to hours, and Amadori products, which form in ~2 days and are often referred to as "early glycation products," could be reclassified as "intermediate glycation products." Schiff bases, Amadori products, and AGEs might represent inherently irreversible (or quasi-irreversible) damage because of their stability, diversity, and/or weak chemical reactivity. This may explain the moderate deglycating efficiencies of fructosamine-3-kinases (27) and AGE breakers (50).

Oxidative Stress Resistance—The involvement of DJ-1 in oxidative stress resistance could be explained by its ability to induce or protect oxidative stress resistance enzymes (3) and protect the thiol proteome against sulfenylation (6). It might also result from interrelations between electrophile and oxidative stresses, as follows: (i) major oxidative stress-resistance proteins, including superoxide dismutases, thioredoxins, glutaredoxins, and peroxidases are inactivated by electrophile stress; (ii) glutathione is hotly contested by proteins involved in electrophile and oxidative stress resistance; and (iii) glycated proteins increase the production of reactive oxygen species (51).

It is debated whether Cys^{106} oxidation to sulfenic or sulfinic acid is incidental, detrimental, or important for cytoprotection by DJ-1 (3). For the repair of sulfenylated and glycated proteins, the reduced form of Cys^{106} is the active form (Ref. 6 and this work), and its low pK_a favors formation of the thiolate anion, which is a more powerful nucleophile than the protonated form. These important functions of DJ-1 in protein repair reduce the probability (although do not eliminate it) of an important role for cysteine 106 oxidation in signaling (3).

Cancer and Apoptosis—The relationship between DJ-1 and cancer is still unclear. A number of reports suggest that DJ-1 is overexpressed in lung, prostate, breast, and pancreatic carcinomas and could be used as a biomarker for tumor diagnosis. We suggest that increased DJ-1 expression in tumors may result from the increased aerobic glycolysis of cancer cells, necessary to meet the metabolic requirements of cell proliferation (52) (the Warburg effect, a characteristic trait of Ras and Myc can-

cers (53)). High glycolytic/HMP rates produce elevated amounts of methylglyoxal and glycated proteins (21), resulting in the overexpression of DJ-1 and avoidance of methylglyoxal-induced toxicity and growth arrest. Glyoxalase 1, thioredoxins, and Nrf2 are also overexpressed in many tumors, providing a growth advantage by increasing chemoresistance or enhancing tumor cell growth (46, 53–55). Such a role for DJ-1 in supporting the viability or proliferation of tumor cells would be sufficient reason to use it as a tumor marker and target for anticancer drug development.

However, several results suggest that DJ-1 may perform more specific functions in cancer or cellular apoptosis. DJ-1 has been described as an oncogene that cooperates with H-Ras or Myc, as a positive effector of the AKT pathway (via PTEN inhibition) and a negative regulator of p53 transcriptional activity (3). DJ-1 was also described as an apoptosis inhibitor, acting by binding the pro-apoptotic proteins Daxx, BCL-X_L, or FADD and by forming a mixed disulfide with the apoptotic regulating kinase ASK1 (3). Several of these results could be explained by the global functions of DJ-1 as a chaperone, a covalent chaperone, a major deglycase, and an anti-stress protein enhancing cell growth. Moreover, the levels of the proapoptotic or tumor-suppressor proteins ASK, PTEN, and p53, which contain active site cysteines (Cys^{250} (ASK), Cys^{124} (PTEN), Cys^{176}, Cys^{238}, and Cys^{242} (p53, zinc binding)) that may physiologically or artifactually react with DJ-1, could also be modified when DJ-1 is overexpressed, consequently generating some of the reported results.

Miscellaneous—Numerous roles for DJ-1 in unrelated functions could be explained by its extensive involvement in protein repair because any protein constitutes a potential DJ-1 substrate. Moreover, the ability of DJ-1 to repair cysteines, lysines, and arginines (frequently encountered in active sites) and the greater sensitivity of active site amino acids to glycation because of their accessibility or shifted pK_a likely increase the occurrence of glycation-induced cellular defects and their correction by DJ-1.

Considering the novel function of DJ-1 and the fact that deglycation obviously constitutes its primary function, we propose that it be renamed DJ-1 deglycase. Although aldoketoreductases, glyoxalases, and multidrug detoxification systems decrease electrophile stressor pools, DJ-1 is a major protein bodyguard, providing front line defense against protein glycation. Finally, the discovery of the deglycase function of DJ-1 may constitute a major advance in biotechnology and for medical research, including aging, neurodegenerative diseases, cancer, atherosclerosis, arterial hypertension, postdiabetic, renal, and autoimmune diseases.

Acknowledgments—We thank Dr. Valerie Gautier for help in the early course of this work, Dr. Sun-Sin Cha for the gift of plasmids coding for wild-type and mutant DJ-1, Dr. Dominique Thierry for critical reading of the manuscript, and Professor Giuseppe Baldacci (Director of the Institut Jacques Monod) for constant support.

REFERENCES

1. Cookson, M. R. (2005) The biochemistry of Parkinson's disease. *Annu. Rev. Biochem.* **74,** 29–52
2. Quigley, P. M., Korotkov, K., Baneyx, F., and Hol, W. G. (2003) The 1.6-A crystal structure of the class of chaperones represented by *Escherichia coli* Hsp31 reveals a putative catalytic triad. *Proc. Natl. Acad. Sci. U.S.A.* **100,** 3137–3142
3. Wilson, M. A. (2011) The role of cysteine oxidation in DJ-1 function and dysfunction. *Antioxid. Redox Signal.* **15,** 111–122
4. Shendelman, S., Jonason, A., Martinat, C., Leete, T., and Abeliovich, A. (2004) DJ-1 is a redox-dependent molecular chaperone that inhibits α-synuclein aggregate formation. *PLoS Biol.* **2,** e362
5. Zhou, W., Zhu, M., Wilson, M. A., Petsko, G. A., and Fink, A. L. (2006) The oxidation state of DJ-1 regulates its chaperone activity toward α-synuclein. *J. Mol. Biol.* **356,** 1036–1048
6. Gautier, V., Le, H. T., Malki, A., Messaoudi, N., Caldas, T., Kthiri, F., Landoulsi, A., and Richarme, G. (2012) YajL, the prokaryotic homolog of the parkinsonism-associated protein DJ-1, protects cells against protein sulfenylation. *J. Mol. Biol.* **421,** 662–670
7. Le, H. T., Gautier, V., Kthiri, F., Malki, A., Messaoudi, N., Mihoub, M., Landoulsi, A., An, Y. J., Cha, S. S., and Richarme, G. (2012) YajL, prokaryotic homolog of Parkinsonism-associated protein DJ-1, functions as a covalent chaperone for thiol proteome. *J. Biol. Chem.* **287,** 5861–5870
8. Andres-Mateos, E., Perier, C., Zhang, L., Blanchard-Fillion, B., Greco, T. M.,Thomas, B., Ko, H. S., Sasaki, M., Ischiropoulos, H., Przedborski, S., Dawson, T. M., and Dawson, V. L. (2007) DJ-1 gene deletion reveals that DJ-1 is an atypical peroxiredoxin-like peroxidase. *Proc. Natl. Acad. Sci. U.S.A.* **104,** 14807–14812
9. Lee, S. J., Kim, S. J., Kim, I. K., Ko, J., Jeong, C. S., Kim, G. H., Park, C., Kang, S. O., Suh, P. G., Lee, H. S., and Cha, S. S. (2003) Crystal structures of human DJ-1 and *Escherichia coli* Hsp31, which share an evolutionarily conserved domain. *J. Biol. Chem.* **278,** 44552–44559
10. Lee JY, Song, J., Kwon, K., Jang, S., Kim, C., Baek, K., Kim, J., and Park, C. (2012) Human DJ-1 and its homologs are novel glyoxalases. *Hum. Mol. Genet.* **21,** 3215–3225
11. Clements, C. M., McNally, R. S., Conti, B. J., Mak, T. W., and Ting, J. P. (2006) DJ-1, a cancer- and Parkinson's disease-associated protein, stabilizes the antioxidant transcriptional master regulator Nrf2. *Proc. Natl. Acad. Sci. U.S.A.* **103,** 15091–15096
12. Junn, E., Taniguchi, H., Jeong, B. S., Zhao, X., Ichijo, H., and Mouradian, M. M. (2005) Interaction of DJ-1 with Daxx inhibits apoptosis signal-regulating kinase 1 activity and cell death. *Proc. Natl. Acad. Sci. U.S.A.* **102,** 9691–9696
13. Guzman, J. N., Sanchez-Padilla, J., Wokosin, D., Kondapalli, J.,Ilijic, E., Schumacker, P. T., and Surmeier, D. J. (2010) Oxidant stress evoked by pacemaking in dopaminergic neurons is attenuated by DJ-1. *Nature* **468,** 696–700
14. van der Brug, M. P., Blackinton, J., Chandran, J., Hao, L. Y., Lal, A., Mazan-Mamczarz, K., Martindale, J., Xie, C., Ahmad, R., Thomas, K. J., Beilina, A., Gibbs, J. R., Ding, J., Myers, A. J., Zhan, M., Cai, H., Bonini, N. M., Gorospe, M., and Cookson, M. R. (2008) RNA binding activity of the recessive Parkinsonism protein DJ-1 supports involvement in multiple cellular pathways. *Proc. Natl. Acad. Sci. U.S.A.* **105,** 10244–10249
15. Hesterkamp, T., and Bukau, B. (1996) The *Escherichia coli* trigger factor. *FEBS Lett.* **389,** 32–34
16. Kern, R., Malki, A., Holmgren, A., and Richarme, G. (2003) Chaperone properties of *E. coli* thioredoxin and thioredoxin reductase. *Biochem. J.* **371,** 965–972
17. Kim, Y. E., Hipp, M. S., Bracher, A., Hayer-Hartl, M., and Hartl, F. U. (2013) Molecular chaperone functions in protein folding and proteostasis. *Annu. Rev. Biochem.* **82,** 323–355
18. Nguyen, T. T., Eiamphungporn, W., Mäder, U., Liebeke, M., Lalk, M., Hecker, M., Helmann, J. D., and Antelmann, H. (2009) Genome-wide responses to carbonyl electrophiles in *Bacillus subtilis*. *Mol. Microbiol.* **71,** 876–894
19. Maillard, L. C. (1912) Action des acides aminés sur les sucres: formation des mélanoïdines par voie méthodique. *C. R. Acad. Sci. Ser.* **2,** 66–68
20. Rahbar, S. (1968) An abnormal hemoglobin in red cells in diabetics. *Clin. Chim. Acta* **22,** 296–298
21. Thornalley, P. J. (2008) Protein and nucleotide damage by glyoxal and methylglyoxal in physiological systems: role in aging and disease. *Drug Metabol. Drug Interact.* **23,** 125–150

22. Thornalley, P. J., and Rabbani, N. (2014) Detection of glycated and oxidized proteins in clinical samples using mass spectrometry: a user's perspective. *Biochim. Biophys. Acta* **1840,** 818–829
23. Jez, J. M., Bennett, M. J., Schlegel, B. P., Lewis, M., and Penning, T. M. (1997) Comparative anatomy of the aldo-keto reductase family. *Biochem. J.* **326,** 625–636
24. Neuberg, C. (1913) The destruction of lactic aldehyde and methylglyoxal by animal organs. *Biochem. Z.* **49,** 502–506
25. Rabbani, N., and Thornalley, P. J. (2012) Methylgloxal, glyoxalase 1 and the dicarbonyl proteome. *Amino Acids* **42,** 1133–1142
26. Smitherman, P. K., Townsend, A. J., Kute, T. E., and Morrow, C. S. (2004) Role of multidrug resistance protein 2 in alkylating agent detoxyfication. *J. Pharmacol. Exp. Ther.* **308,** 260–267
27. Van Schaftingen, E., Collard, F., Wiame, E., and Veiga-da-Cunha, M. (2012) Enzymatic repair of Amadori products. *Amino acids* **42,** 1143–1150
28. Kthiri, F., Le, H. T., Gautier, V., Caldas, T., Malki, A., Landoulsi, A., Bohn, C., Bouloc, P., and Richarme, G. (2010) Protein aggregation in a mutant deficient in YajL, the bacterial homolog of the Parkinsonism-associated protein DJ-1. *J. Biol. Chem.* **285,** 10328–10336
29. Lo, T. W., Westwood, M. E., McLellan, A. C., Selwood, T., and Thornalley, P. J. (1994) Binding and modification of proteins by methylglyoxal under physiological conditions: a kinetic and mechanistic study with N^{α}-acetylarginine, N^{α}-acetylcysteine, and N^{α}-acetyllysine, and bovine serum albumin. *J. Biol. Chem.* **269,** 32299–32305
30. Morgan, P. E., Dean, R. T., and Davies, M. J. (2002) Inactivation of cellular enzymes by carbonyls and protein-bound glycation/glycoxidation products. *Arch. Biochem. Biophys.* **403,** 259–269
31. McLaughlin, J. A., Pethig, R., and Szent-Györgyi, A. (1980) Spectroscopic studies of the protein-methylglyoxal adduct. *Proc. Natl. Acad. Sci. U.S.A.* **77,** 949–951
32. Patthy, L., and Smith, E. L. (1975) Identification of functional arginines residues in ribonulclease A and lysozyme. *J. Biol. Chem.* **250,** 565–569
33. Leoncini, G., Ronchi, S., Maresca, M., and Bonsignore, A. (1980) Studies of the interaction of fructose 1,6-P2 aldolase with methylglyoxal. *Ital. J. Biochem.* **29,** 289–299
34. Seidler, N. W., and Kowalewski, C. (2003) Methylglyoxal-induced glycation affects protein topography. *Arch. Biochem. Biophys.* **410,** 149–154
35. Messaoudi, N., Gautier, V., Kthiri, F., Lelandais, G., Mihoub, M., Joseleau-Petit, D., Caldas, T., Bohn, C., Tolosa, L., Rao, G., Tao, K., Landoulsi, A., Bouloc, P., and Richarme, G. (2013) Global stress response in a prokaryotic model of DJ-1-associated Parkinsonism. *J. Bacteriol.* **195,** 1167–1178
36. Bretes, H., Rouviere, J. O., Leger, T., Oeffinger, M., Devaux F., Doye, V., and Palancade, B. (2014) Sumoylation of the THO complex regulates the biogenesis of a subset of mRNPS. *Nucleic Acids Res.* **42,** 5043–5058
37. Richarme, G. (1983) Associative properties of the *Escherichia coli* galactose-binding protein and maltose-binding protein. *Biochim. Biophys. Acta* **748,** 99–108
38. Malki, A., Kern, R., Abdallah, J., and Richarme, G. (2003) Characterization of the *Escherichia coli* YedU protein as a molecular chaperone. *Biochem. Biophys. Res. Commun.* **301,** 430–436
39. Abdallah, J., Caldas, T., Kthiri, F., Kern, R., and Richarme, G. (2007) YhbO protects cells against multiple stresses. *J. Bacteriol.* **189,** 9140–9144
40. Malki, A., Caldas, T., Abdallah, J., Kern, R., Eckey, V., Kim, S. J., Cha, S. S., Mori, H., and Richarme, G. (2005) Peptidase activity of the *Escherichia coli* Hsp31 chaperone. *J. Biol. Chem.* **280,** 14420–14426
41. Sastry, M. S., Korotkov, K., Brodsky, Y., and Baneyx, F. (2002) Hsp31, the *Escherichia coli yedU* gene product, is a molecular chaperone whose activity is inhibited by ATP at high temperatures. *J. Biol. Chem.* **277,** 46026–46034
42. Wilson, M. A., Ringe, D., and Petsko, G. A. (2005) The atomic resolution crystal structure of the YajL protein from *Escherichia coli*: a close prokaryotic homologue of the Parkinsonism-associated protein DJ-1. *J. Mol. Biol.* **353,** 678–691
43. Pepper, E. D., Farrell, M. J., Nord, G., and Finkel, S. E. (2010) Antiglycation effects of carnosine and other compounds on the long-term survival of *Escherichia coli*. *Appl. Environ. Microbiol.* **76,** 7925–7930
44. Mironova, R., Niwa, T., Hayashi, H., Dimitrova, R., and Ivanov, I. (2001) Evidence for non-enzymatic glycosylation in *Escherichia coli*. *Mol. Microbiol.* **39,** 1061–1068
45. Chen, J., Li, L., and Chin, L. S. (2010) Parkinson disease protein DJ-1 converts from a zymogen to a protease by carboxyl-terminal cleavage. *Hum. Mol. Genet.* **19,** 2395–2408
46. Thornalley, P. J., and Rabbani, N. (2011) Glyoxalase in tumourigenesis and multidrug resistance. *Semin. Cell Dev. Biol.* **22,** 318–325
47. Szwergold, B. S., Howell, S. K., and Beisswenger, P. J. (2005) Transglycation, a potential new mechanism for deglycation of Schiff bases. *Ann. N.Y. Acad. Sci.* **1043,** 845–864
48. Li, J., Liu, D., Sun, L., Lu, Y., Zhang, Z. (2012) Advanced glycation end products and neurovegetative diseases: mechanisms and perspectives. *J. Neurol. Sci.* **317,** 1–5
49. Vicente Miranda, H., and Outeiro, T. F. (2010) The sour side of neurovegetative disorders: the effects of protein glycation. *J. Pathol.* **221,** 13–25
50. Yamagishi, S. (2012) Potential clinical utility of advanced glycation product cross-link breakers in age- and diabetes-associated disorders. *Rejuvenation Res.* **15,** 564–572
51. Ma, Q. (2013) Role of Nrf2 in oxidative stress and toxicity. *Annu. Rev. Pharmacol. Toxicol.* **53,** 401–426
52. Lunt, S. Y., and Vander Heiden, M. G. (2011) Aerobic glycolysis: meeting the metabolic requirements of cell proliferation. *Annu. Rev. Cell Dev. Biol.* **27,** 441–464
53. Hanahan, D., and Weinberg, R. A. (2011) Hallmarks of cancer: the next generation. *Cell* **144,** 646–674
54. Kansanen, E., Kuosmanen, S. M., Leinonen, H., and Levonen, A. L. (2013) The Keap-1-Nrf2 pathway: mechanisms of activation and dysregulation in cancer. *Redox Biol.* **1,** 45–49
55. Lu, J., and Holmgren, A. (2012) Thioredoxin system in cell death progression. *Antioxid. Redox Signal.* **17,** 1738–1747